



Performance Evaluation of Blind Image Quality Assessment on Deconvolving Images

R.Likhitha¹, K.Ramesh²

¹M.Tech Student, Dept. Of Electronics & Communication Engineering, Sree Vidyanikethan Engineering College, Tirupati, AP, India

²M.Tech, Assistant Professor, Dept. Of Electronics & Communication Engineering, Sree Vidyanikethan Engineering College, Tirupati, AP, India

ABSTRACT: We develop an efficient general-purpose blind/no-reference image quality assessment (IQA) algorithm using a natural scene statistics (NSS) model of discrete cosine transform (DCT) coefficients. The algorithm is computationally appealing, given the availability of platforms optimized for DCT computation. The approach relies on a simple Bayesian inference model to predict image quality scores given certain extracted features. The features are based on an NSS model of the image DCT coefficients. The estimated parameters of the model are utilized to form features that are indicative of perceptual quality. These features are used in a simple Bayesian inference approach to predict quality scores. The resulting algorithm, which we name BLIINDS-II, requires minimal training and adopts a simple probabilistic model for score prediction. Given the extracted features from a test image, the quality score that maximizes the probability of the empirically determined inference model is chosen as the predicted quality score of that image. When tested on the LIVE IQA database, BLIINDS-II is shown to correlate highly with human judgments of quality, at a level that is competitive with the popular SSIM index.

I.INTRODUCTION

The ubiquity of transmitted digital visual information in daily and professional life, and the broad range of applications that rely on it, such as personal digital assistants, high-definition televisions, internet video streaming, and video on demand, necessitate the means to evaluate the visual quality of this information. The various stages of the pipeline through which an image passes can introduce distortions to the image, beginning with its capture until its consumption by a viewer. The acquisition, digitization, compression, storage, transmission, and display processes all introduce modifications to the original image.

Only recently did full-reference image quality assessment (FR-IQA) methods reach a satisfactory level of performance, as demonstrated by high correlations with human subjective judgments of visual quality. SSIM, MS-SSIM, VSNR, VIF index, and the divisive normalization-based indices in and are examples of successful FR-IQA algorithms. These methods require the availability of a reference signal against which to compare the test signal. In many applications, however, the reference signal is not available to perform a comparison against. This strictly limits the application domain of FR-IQA algorithms and points to the need for reliable blind/NR-IQA algorithms. However, no NR-IQA algorithm has been proven consistently reliable in performance. While some FR-IQA algorithms are reliable enough to be deployed in standards, generic NR-IQA algorithms have been regarded as having a long way to go before reaching similar useful levels of performance. The problem of blindly assessing the visual quality of images, in the absence of a reference, and without assuming a single distortion type, requires dispensing with older ideas of quality such as fidelity, similarity, and metric comparison. Presently, NR-IQA algorithms generally follow one of three trends: 1) distortion-specific approaches. These employ a specific distortion model to drive an objective algorithm to predict a subjective quality score. These algorithms quantify one or more distortions such as blockiness, blur, or ringing and score the image accordingly; 2) training based approaches: these train a model to predict the image quality score based on a number of features extracted from



International Journal of Advanced Research in Electrical, Electronics and Instrumentation Engineering

(An ISO 3297: 2007 Certified Organization)

Vol. 3, Issue 8, August 2014

the image ; and 3) natural scene statistics (NSS) approaches: these rely on the hypothesis that images of the natural world (i.e., distortion-free images) occupy a small subspace of the space of all possible images and seek to find a distance between the test image and the subspace of natural images To perform the JPEG coding, an image (in colour or grey scales) is first subdivided into blocks of 8x8 pixels. The Discrete Cosine Transform (DCT) is then performed on each block. This generates 64 coefficients which are then quantised to reduce their magnitude. The coefficients are then reordered into a one-dimensional array in a zigzag manner before further entropy encoding. The compression is achieved in two stages; the first is during quantisation and the second during the entropy coding process. JPEG decoding is the reverse process of coding.

II. EXISTING METHOD

The alternating direction method of multipliers (ADMM), originally proposed in the 1970's, emerged recently as a flexible and efficient tool for several imaging inverse problems, such as denoising , deblurring, inpainting, reconstruction, motion segmentation, to mention only a few classical problems. ADMM-based approaches make use of variable splitting, which allows a straightforward treatment of various priors/regularizers, such as those based on frames or on *total-variation* (TV), as well as the seamless inclusion of several types of constraints. ADMM is closely related to other techniques, namely the so-called *Bregman* and *split Bregman* methods and *Douglas-Rachford splitting*. Several ADMM-based algorithms for imaging inverse problems require, at each iteration, solving a linear system (equivalently, inverting a matrix). As illustrated in Figure 1, all these standard BCs are quite unnatural, as they do not correspond to any realistic imaging system, being motivated merely by computational convenience. Namely, assuming a periodic boundary condition has the advantage of allowing a very fast implementation of the convolution as a point-wise multiplication in the DFT



Fig. 1. Illustration of the (unnatural) assumptions underlying the periodic, reflexive, and zero boundary conditions.

domain, efficiently implementable using the FFT. However, in real problems, there is no reason for the external (unobserved) pixels to follow periodic (or any other) boundary conditions. A well known consequence of this mismatch is a degradation of the deconvolved images, such as the appearance of ringing artifacts emanating from the boundaries. These artifacts can be reduced by pre-processing the image to reduce the spurious discontinuities at the boundaries, created by the (wrong) periodicity assumption; this is what is done by the “edgetaper” function in the MATLAB Image Processing Toolbox. In a more sophisticated version of this idea that was recently proposed, the observed image is extrapolated to create a larger image with smooth BCs

Algorithm 1: ADMM

```

1 Initialization: set  $k = 0$ , choose  $\mu > 0$ ,  $\mathbf{u}_0$ , and  $\mathbf{d}_0$ .
2 repeat
3    $\mathbf{z}_{k+1} \leftarrow \arg \min_{\mathbf{z}} f(\mathbf{z}) + \frac{\mu}{2} \| \mathbf{G} \mathbf{z} - \mathbf{u}_k - \mathbf{d}_k \|_2^2$ 
4    $\mathbf{u}_{k+1} \leftarrow \arg \min_{\mathbf{u}} g(\mathbf{u}) + \frac{\mu}{2} \| \mathbf{G} \mathbf{z}_{k+1} - \mathbf{u} - \mathbf{d}_k \|_2^2$ 
5    $\mathbf{d}_{k+1} \leftarrow \mathbf{d}_k - (\mathbf{G} \mathbf{z}_{k+1} - \mathbf{u}_{k+1})$ 
6    $k \leftarrow k + 1$ 
7 until stopping criterion is satisfied

```



International Journal of Advanced Research in Electrical, Electronics and Instrumentation Engineering

(An ISO 3297: 2007 Certified Organization)

Vol. 3, Issue 8, August 2014

Algorithm 2: ADMM-2

```

1 Initialization: set  $k = 0$ , choose  $\mu_1, \dots, \mu_J > 0$ ,  $\mathbf{u}_0, \mathbf{d}_0$ .
2 repeat
3    $\zeta \leftarrow \mathbf{u}_k + \mathbf{d}_k$ 
4    $\mathbf{z}_{k+1} \leftarrow \left( \sum_{j=1}^J \mu_j (\mathbf{H}^{(j)})^* \mathbf{H}^{(j)} \right)^{-1} \sum_{j=1}^J \mu_j (\mathbf{H}^{(j)})^* \zeta^{(j)}$ 
5   for  $j = 1$  to  $J$  do
6      $\mathbf{u}_{k+1}^{(j)} \leftarrow \text{PROX}_{g_j/\mu_j}(\mathbf{H}^{(j)} \mathbf{z}_{k+1} - \mathbf{d}_k^{(j)})$ 
7      $\mathbf{d}_{k+1}^{(j)} \leftarrow \mathbf{d}_k^{(j)} - (\mathbf{H}^{(j)} \mathbf{z}_{k+1} - \mathbf{u}_{k+1}^{(j)})$ 
8   end
9    $k \leftarrow k + 1$ 
10 until stopping criterion is satisfied
  
```

III. PROPOSED METHOD

Our approach relies on the IQA algorithm learning how the NSS model parameters vary across different perceptual levels of image distortion. The algorithm is trained using features derived directly from a generalized parametric statistical model of natural image DCT coefficients against various perceptual levels of image distortion. The learning model is then used to predict perceptual image quality scores. Unlike much of the prior work on image/video quality assessment (QA) .We make little direct use of specific perceptual models such as area cortical decompositions , masking and motion perception. Yet we consider our approach as perceptually relevant since the NSS models reflect statistical properties of the world that drive perceptual functions of the HVS. This is a consequence of the belief that the HVS is adapted to the statistics of its visual natural environment. In other words, models of natural scenes embody characteristics of the HVS, which is hypothesized to be evolutionally adapted to models conforming to natural scenes. HVS characteristics that are intrinsic to, or that can be incorporated into NSS models include: 1) visual sensitivity to structural information; 2) perceptual masking ; 3) visual sensitivity to directional information ; 4) multi scale spatial visual processing ; and 5) intolerance to flagrantly visible visual distortions . In the following sections we explain how one or more of these HVS properties are embedded in the model. The generalized Gaussian model has recently been used as afeature in a NSS-based RR-IQA algorithm and in a simpletwo-stage NR-IQA algorithm .

The univariate generalized Gaussian density is given by

$$f(x|\alpha, \beta, \gamma) = \alpha e^{-(\beta|x-\mu|)^\gamma} \quad (1)$$

$$\alpha = \frac{\beta\gamma}{2\Gamma(1/\gamma)} \quad (2)$$

where μ is the mean, γ is the shape parameter, and α and β are the normalizing and scale parameters given by

$$\beta = \frac{1}{\sigma} \sqrt{\frac{\Gamma(3/\gamma)}{\Gamma(1/\gamma)}} \quad (3)$$

where σ is the standard deviation, and Γ denotes the gamma function given by

$$\Gamma(z) = \int_0^\infty t^{z-1} e^{-t} dt. \quad (4)$$

International Journal of Advanced Research in Electrical, Electronics and Instrumentation Engineering

(An ISO 3297: 2007 Certified Organization)

Vol. 3, Issue 8, August 2014

This family of distributions includes the Gaussian distribution ($\beta = 2$) and the Laplacian distribution ($\beta = 1$). As $\beta \rightarrow \infty$, the distribution converges to a uniform distribution. The GGD at varying levels of the shape parameter γ . A variety of parameter estimation methods have been proposed for this model. The multivariate version of the generalized Gaussian density is given by

$$f(x|\alpha, \beta, \gamma) = \alpha e^{-(\beta(x-\mu)^T \Sigma^{-1}(x-\mu))^\gamma} \quad (5)$$

Visual images are subjected to local spatial frequency decompositions in the visual cortex. Likewise, in our IQA model, feature extraction is performed in the local frequency (DCT) domain. The main motivation behind feature extraction in the DCT domain is the observation that the statistics of DCT coefficients change with the degree and type of image distortion. Another advantage is computational convenience: optimized DCT-specific platforms, and fast algorithms for DCT computation, can ease computation. For instance, DCTs can be computed efficiently by variable-change transforms from computationally efficient fast Fourier transform algorithms. Many image and video compression algorithms are based on block-based DCT transforms (JPEG, MPEG2, H263, and H264 that relies on a variation of the DCT). Consequently, the model-based method could be applied to already-computed coefficients, resulting in even greater computational efficiency. Finally, and perhaps most importantly, it is possible to define simple and naturally defined model-based DCT features that capture perceptually relevant image and distortion characteristics in a natural and convenient manner. We illustrate one instance of how the statistics of DCT coefficients changes as an image becomes distorted, which shows the DCT coefficient histograms of a distortion-free image and a Gaussian blur distorted image, respectively. The differences in observed DCT coefficient distributions between distorted and non distorted images are exploited in the design of features of visual quality score prediction.

IV. EXPERIMENTAL RESULTS

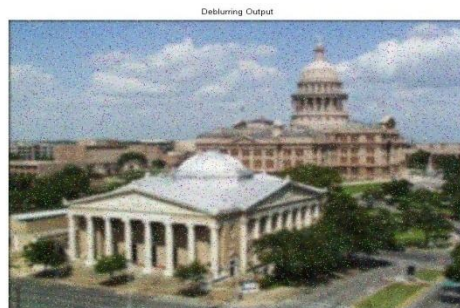


Fig.1. Deblurring output

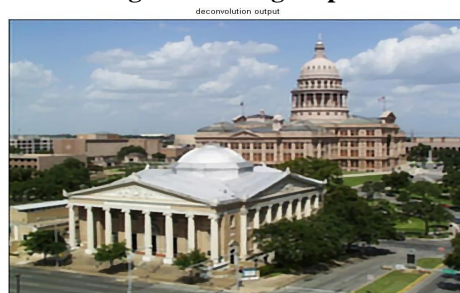


Fig.2. Deconvolution output

International Journal of Advanced Research in Electrical, Electronics and Instrumentation Engineering

(An ISO 3297: 2007 Certified Organization)

Vol. 3, Issue 8, August 2014

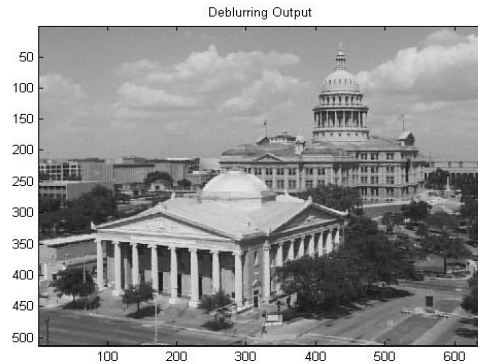


Fig.3.Deblurring output

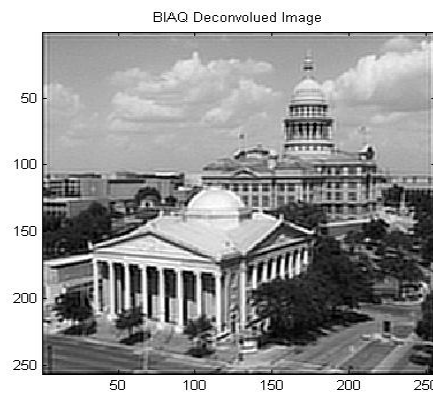


Fig.4.BIAQ Deconvolution Image

Table for comparing Improved SNR values for different algorithms with present method

| | TV-BC | TV-ET | TV-CG | TV-MD | BIQA |
|------|-------|-------|-------|-------|-------|
| BSNR | | | | | |
| 30dB | 1.39 | 2.42 | 2.44 | 3.04 | 4.01 |
| 40dB | 1.46 | 3.11 | 3.44 | 3.59 | 4.62 |
| 50dB | 2.97 | 4.91 | 6.34 | 6.31 | 7.96 |
| 60dB | 8.27 | 15.94 | 16.08 | 25.75 | 28.13 |

(a)



International Journal of Advanced Research in Electrical, Electronics and Instrumentation Engineering

(An ISO 3297: 2007 Certified Organization)

Vol. 3, Issue 8, August 2014

| | FA-BC | FA-ET | FA-CG | FA-MD | BIQA |
|------|-------|-------|-------|-------|-------|
| BSNR | | | | | |
| 30dB | -0.20 | 2.89 | 1.84 | 3.16 | 3.69 |
| 40dB | -2.15 | 2.62 | 3.65 | 4.18 | 4.71 |
| 50dB | -2.97 | 4.92 | 5.57 | 6.92 | 7.69 |
| 60dB | -8.49 | 15.32 | 16.20 | 25.48 | 27.56 |

(b)

(a)-(b) Improved SNR values

V. CONCLUSION

The main limitation of these types of “learning based” algorithms is that they require training to learn the prediction parameters (i.e., they suffer regression limitations). Consequently, if these algorithms are trained on a subset (of all possible) image distortions, then these algorithms are expected to perform well on the distortions they have encountered during training, or on distortions that affect images in a similar manner to the ones encountered during training. We leave the design of effective no-reference methods that are completely non reliant on training as challenging future work.

There are significant design differences between DIIVINE and BLIINDS-II. DIIVINE uses a dense complex representation of images in the wavelet domain and extracts a large number of features to train two stages of the algorithm: 1) a nonlinear SVM training for classification and 2) a nonlinear SRV training for regression within each class. Given M assumed distortions, DIIVINE requires M distortion-specific quality assessment engines to be trained and applied. Hence, DIIVINE does not directly accomplish multi distortion QA. Instead, it computes a probability. There are significant design differences between DIIVINE and BLIINDS-II. DIIVINE uses a dense complex representation of images in the In addition, the DIIVINE index and the BLIINDS index target essentially different application domains. The DIIVINE index, by a two-stage strategy, enables the identification of distortions afflicting the image. This is not only valuable for accomplishing directed quality assessment but also for iden SAAD.: BLIND IMAGE QUALITY ASSESSMENT 3351 tifying image distortions to be repaired. This is accomplished at considerable computational expense using a much larger feature set and sophisticated learning mechanisms. By comparison, the BLIINDS index is designed to achieve the speed and performance required by a quality assessment algorithm operating in a high speed video network. It accomplishes this via a simple one-stage QA process using a small number of NSS features that are easily computed from a small (subsamped) number of fast DCT coefficients, using a very simple probabilistic classifier. In the future, we envision NSS-based QA algorithms that use spatiotemporal features for *video*-QA and NSS-depth features for *stereo*-QA. These may efficiently operate in the DCT domain like BLIINDS-II.

REFERENCES

- [1] Q. Li and Z. Wang, “Reduced-reference image quality assessment using divisive-normalization-based image representation,” *IEEE J. Sel. Topics Signal Process.*, vol. 3, no. 2, pp. 202–211, Apr. 2009.
- [2] J. Malo and V. Laparra, “Psychophysically tuned divisive normalization approximately factorizes the PDF of natural images,” *Neural Comput.*, vol. 22, no. 12, pp. 3179–3206, 2010.
- [3] A. K. Moorthy and A. C. Bovik, “Visual importance pooling for image quality assessment,” *IEEE J. Sel. Topics Signal Process.*, vol. 3, no. 2, pp. 193–201, Apr. 2009.
- [4] K. Seshadrinathan and A. C. Bovik, “Motion tuned spatio-temporal quality assessment of natural videos,” *IEEE Trans. Image Process.*, vol. 19, no. 2, pp. 335–350, Feb. 2010.
- [5] G. E. Legge and J. M. Foley, “Contrast masking in human vision,” *J. Opt. Soc. Amer.*, vol. 70, no. 12, pp. 1458–1471, 1980.



ISSN (Print) : 2320 – 3765
ISSN (Online): 2278 – 8875

International Journal of Advanced Research in Electrical, Electronics and Instrumentation Engineering

(An ISO 3297: 2007 Certified Organization)

Vol. 3, Issue 8, August 2014

- [6] H. B. Barlow, "Redundancy reduction revisited," *Netw. Comput. Neural Syst.*, vol. 12, no. 3, pp. 241–253, 2001.
- [7] S. Gabarda and G. Cristobal, "Blind image quality assessment through anisotropy," *J. Opt. Soc. Amer.*, vol. 24, no. 12, pp. B42–B51, Dec. 2007.
- [8] W. S. Geisler and J. S. Perry, "Contour statistics in natural images: Grouping across occlusions," *Visual Neurosci.*, vol. 26, no. 1, pp. 109–121, 2009.
- [9] A. K. Moorthy and A. C. Bovik, "Perceptually significant spatial pooling strategies for image quality assessment," *Proc. SPIE Human Vis. Electron. Imag.*, vol. 7240, pp. 724012-1–724012-11, Jan. 2009.
- [10] A. Srivastava, A. B. Lee, E. P. Simoncelli, and S. C. Zhu, "On advances in statistical modeling of natural images," *J. Math. Imag. Vision*, vol. 18, no. 1, pp. 17–33, 2003.
- [11] H. R. Sheikh, A. C. Bovik, and G. De Veciana, "An information fidelity criterion for image quality assessment using natural scene statistics," *IEEE Trans. Image Process.*, vol. 14, no. 12, pp. 2117–2128, Dec. 2005.
- [12] A. C. Bovik, T. S. Huang, and D. C. Munson, "A generalization of median filtering using linear combinations of order statistics," *IEEE Trans. Acoust. Speech Signal Process.*, vol. 31, no. 6, pp. 1342–1350, Dec. 1983.
- [13] H. G. Longbotham and A. C. Bovik, "Theory of order statistic filters and their relationship to linear FIR filters," *IEEE Trans. Acoust. Speech Signal Process.*, vol. 37, no. 2, pp. 275–287, Feb. 1989.
- [14] K. Sharifi and A. Leon-Garcia, "Estimation of shape parameter for generalized gaussian distributions in sub band decompositions of video," *IEEE Trans. Circuits Syst. Video Technol.*, vol. 5, no. 1, pp. 52–56, Feb. 1995.
- [15] A. C. Bovik, M. Clark, and W. S. Geisler, "Multichannel texture analysis using localized spatial filters," *IEEE Trans. Pattern Anal. Mach. Intell.*, vol. 12, no. 1, pp. 55–73, Jan. 1990.
- [16] Y. Shain, A. Akerib, and R. Adar, "Associative architecture for fast DCT," in *Proc. IEEE Int. Conf. Acoust. Speech Signal Process.*, May 1998, pp. 3109–3112.
- [17] J. Huan, M. Parris, J. Lee, and R. F. DeMara, "Scalable FPGA-based architecture for DCT computation using dynamic partial reconfiguration," *ACM Trans. Embedded Comput. Syst.*, vol. 9, no. 1, pp. 1–18, Oct. 2009.
- [18] S. Balam and D. Schonfeld, "Associative processors for video coding applications," *IEEE Trans. Circuits Syst. Video Technol.*, vol. 16, no. 2, pp. 241–250, Feb. 2006.
- [19] P. Duhamel, C. Guillemot, and J. C. Carlach, "A DCT chip based on a new structured and computationally efficient DCT algorithm," in *Proc. IEEE Int. Symp. Circuits Syst.*, May 1990, pp. 77–80.
- [20] N. I. Cho and S. U. Lee, "Fast algorithm and implementation of 2-D discrete cosine transform," *IEEE Trans. Circuits Syst.*, vol. 38, no. 3, pp. 297–305, Mar. 1991.
- [21] M. Haque, "A 2-D fast cosine transform," *IEEE Trans. Acoust. Speech Signal Process.*, vol. 33, no. 6, pp. 1532–1539, Dec. 1985.
- [22] N. Bozinovic and J. Konrad, "Motion analysis in 3D DCT domain and its application to video coding," *Signal Process. Image Commun.*, vol. 20, no. 6, pp. 510–528, Jul. 2005.
- [23] H. R. Sheikh, Z. Wang, L. Cormack, and A. C. Bovik. *LIVE Image Quality Assessment Database Release 2* [Online]. Available: <http://live.ece.utexas.edu/research/quality>
- [24] N. Ponomarenko, V. Lukin, A. Zelensky, K. Egiazarian, M. Carli, and F. Battisti, "TID 2008 a database for evaluation of full-reference visual quality assessment metrics," *Adv. Modern Radioelectron.*, vol. 10, pp. 30–45, 2009.
- [25] M. H. Pinson and S. Wolf, "A new standardized method for objectively measuring video quality," *IEEE Trans. Broadcast.*, vol. 10, no. 3, pp. 312–322, Sep. 2004.